Vibration and Impact in Multigirder Steel Bridges

TON-LO WANG, DONGZHOU HUANG, AND MOHSEN SHAHAWY

Vibration and impact due to multiple vehicles moving across rough bridge decks are studied in seven steel multigirder bridges with different span lengths. The bridges are modeled as grillage beam systems. The vehicle is simulated as a nonlinear vehicle model with 12 degrees of freedom according to the HS20-44 truck design loading specified by AASHTO. Four classes of road surface roughness generated from power spectral density function for the approach roadways and bridge decks are used in the analysis. The results indicate that the impact of exterior girders of short-span bridges are highly sensitive to lateral loading position, vehicle weight, road roughness, and so forth. Maximum impact factors of girders were obtained for two trucks (side by side) through changing their transverse positions, with different speeds and road surface roughness. Results are useful for the bridge design and the further study of impact formula proposed by AASHTO.

The impact on highway bridges of vehicles passing across the spans is a significant problem of interest to bridge engineers. A considerable amount of literature exists on this subject. The literature most relevant to this study concerns code provisions, experimental impact values, and the models for vehicles and bridges used in analytical studies.

The 1989 AASHTO specifications (*1*) are the basis for the design of highway bridges in many countries. They specify

$$I = \frac{50}{(L + 125)} \tag{1}$$

where I is an impact factor not greater than 0.3, and L is the loaded length in feet. The 1983 Ontario Bridge Design Code (*2*) has introduced more conservative values of I.

In the past two decades, many experimental studies reported that high impact occurred in some highway bridges (*3–7*). Many papers on the theoretical study of the dynamic loading of girder bridges have been published during the past three decades (*8–11*). The theoretical and experimental investigations indicate that the impact of a bridge depends on many factors: (a) the type of bridge and its natural frequencies of vibration, (b) vehicle characteristics, (c) speed of the vehicle, (d) the profile of approach roadway and of bridge deck, (e) the damping characteristics of bridge and vehicle, (f) weight of the vehicle, and so forth.

However, most of these previous studies used a planar beam model or orthotropic model to simulate bridge structure and a single car to simulate vehicle loading. A recent investigation by Wang and Huang (*12,13*) has shown that the impact of bridges was greatly influenced by the wheel-load distribution, and the impact of each girder is not same. Nevertheless, a thorough investigation on this subject needs to be conducted.

The present objective is to analyze systematically the vibration and impact of multigirder steel bridges with seven span lengths from 35 to 140 ft (10.67 to 42.67 m), under the passage of design vehicle loading. The results obtained are useful for further theoretical and field study of bridge impact as well as for modification of highway bridge design specifications.

MATHEMATICAL MODEL FOR VEHICLE

The mathematical model for HS20-44 truck loading is illustrated in Figure 1. The nonlinear vehicle model consists of five rigid masses representing the tractor, semitrailer, steer wheel/axle set, tractor wheel/axle set, and trailer wheel/axle set, respectively. In the model, the tractor and semitrailer were each assigned 3 degrees of freedom (df), corresponding to the vertical displacement (y), rotation about the transverse axis (pitch, or θ), and rotation about the longitudinal axis (roll, or ϕ). Each wheel/axle set is provided with two df in the vertical and roll directions. The total degrees of freedom are 12. The tractor and semitrailer were interconnected at the pivot point (the so-called fifth wheel point; see Figure 1). Both distances between the steer axle and the tractor axle as well as the tractor axle and the trailer axle are taken as 14 ft (4.27 m). The equations of motion of the system were derived by using Lagrange's formulation. Details of derivation and data are discussed by Wang and Huang (*13*).

ROAD SURFACE ROUGHNESS

The power spectral density (PSD) functions for highway surface roughness have been developed by Dodds and Robson (*14*) and modified by Wang and Huang (*13*). They are shown as

$$S(\bar{\phi}) = A_r \left(\frac{\bar{\phi}}{\bar{\phi}_0}\right)^{-2} \tag{2}$$

where

$S(\bar{\phi})$ = PSD (m^2/cycle/m)
$\bar{\phi}$, = wave number (cycle/m),

T.-L. Wang, D. Z. Huang, Department of Civil and Environmental Engineering, Florida International University, Miami, Fla. 33199. M. Shahawy, Structures Research and Testing Center, Florida Department of Transportation, Tallahassee, Fla. 32310.

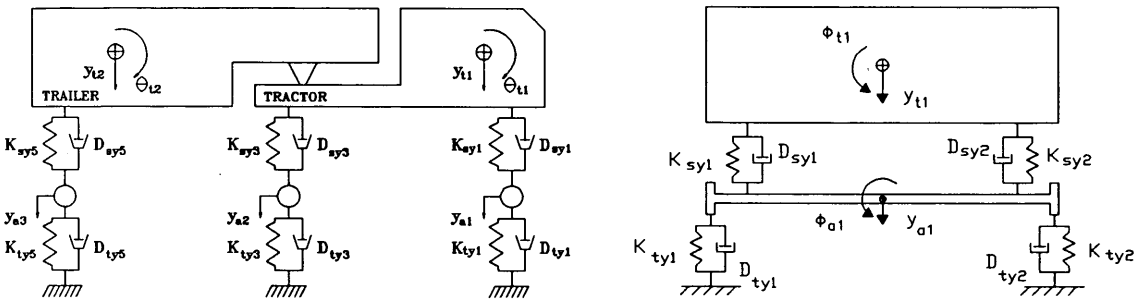

FIGURE 1 HS20-44 vehicle model: *left*, side view; *right*, front view.

A_r = roughness coefficient (m^3/cycle)
$\overline{\Phi}_0$ = discontinuity frequency = $1/(2\pi)$ (cycle/m).

The detail of the procedure has been discussed by Wang and Huang (*13*). In this study, the values of 5×10^{-6}, 20×10^{-6}, 80×10^{-6}, and 256×10^{-6} m^3/cycle were used according to International Organization for Standardization (ISO) specifications (*15*) as the roughness coefficient A_r for the classes of very good, good, average, and poor roads, respectively. The sample length was taken as 256 m (839.9 ft), and 2,048 (2^{11}) data points were generated for this distance. The average vertical highway surface profiles from five simulations are shown in Figure 2.

BRIDGE MODEL AND EQUATIONS OF MOTION

To study the general impact behavior of steel multigirder bridges, seven highway steel bridges were designed according to 1989 AASHTO specifications (*1*) and the 1982 Standard Plans for Highway Bridges of the U.S. Department of Transportation (*16*). The span lengths range from 35 to 140 ft (10.67 to 42.67 m). These bridges are designed for the HS20-44 loading. Figure 3 (*top*) shows the typical bridge cross section. All seven bridges consist of five identical girders that are simply supported. The plan of the bridge with a span of 100 ft is given in Figure 3 (*bottom*); the other bridges have similar arrangements. The number of diaphragms for bridges with span lengths of 35, 45, 55, 75, 100, 120, and 140 ft (1 ft = 0.305 m) are 1, 1, 2, 2, 3, 4, and 5, respectively. The primary bridge data are given in Table 1.

The multigirder bridges are treated as grillage beam systems (Figure 4). Dynamic response of the bridge was analyzed with finite element method. The bridge was divided into grillage elements (Figure 5). The node parameters are

$$\{\delta\}^e = \begin{Bmatrix} \delta_i \\ \delta_j \end{Bmatrix} \tag{3}$$

where

$\{\delta_i\} = [w_{zi}\ \theta_{xi}\ \theta_{yi}]^T$ = displacement vector of left joint,
$\{\delta_j\} = [w_{zj}\ \theta_{xj}\ \theta_{yj}]^T$ = displacement vector of right joint,
w = vertical displacement in z-direction, and
θ_x, θ_y = rotational displacements about x- and y-axes, respectively.

The equations of motion of the bridge are

$$[M_B]\{\ddot{\delta}\} + [D_B]\{\dot{\delta}\} + [K_B]\{\delta\} = \{F_{BT}\} \tag{4}$$

where

$[M_B]$ = global mass matrix;
$[K_B]$ = global stiffness matrix;
$[D_B]$ = global damping matrix;
$\{\delta\}$, $\{\dot{\delta}\}$, $\{\ddot{\delta}\}$ = global nodal displacement, velocity, acceleration vectors; and
$\{F_{BT}\}$ = global nodal loading vector, resulting from interaction between bridge and vehicle.

INTERACTION EQUATIONS AND NUMERICAL METHODS

The interaction force of the ith axle between the bridge and vehicle is given as

$$F^i_{BT} = K_{tyi}U_{tyi} + D_{tyi}\dot{U}_{tyi} \tag{5}$$

where

K_{tyi} = tire stiffness of ith axle,
D_{tyi} = tire damping coefficient of ith axle, and
U_{tyi} = relative displacement between ith axle and bridge $= y_{si} - (-u_{sri}) - (-w_{bi})$, where y_{ai} = vertical displacement of ith axle,
u_{sri} = road surface roughness under ith axle (positive upward), and
w_{bi} = bridge vertical displacement under ith axle (positive upward); w_{bi} can be evaluated by nodal displacements $\{\delta\}^e$ of element and displacement interpolation function of element (*12*); a dot superscript denotes differential with respect to time.

The equations of motion of the vehicle are nonlinear, while those of the bridge are considered linear. According to the different characteristics of the equations of motion, the fourth-order Runge-Kutta integration scheme (*17*) was used to solve the equations of motion of the vehicle, while the solutions of those of the bridge were determined by the mode-superposition procedure based on the subspace iteration method. The main procedure for dynamic analysis of the bridges is discussed elsewhere (*12*).

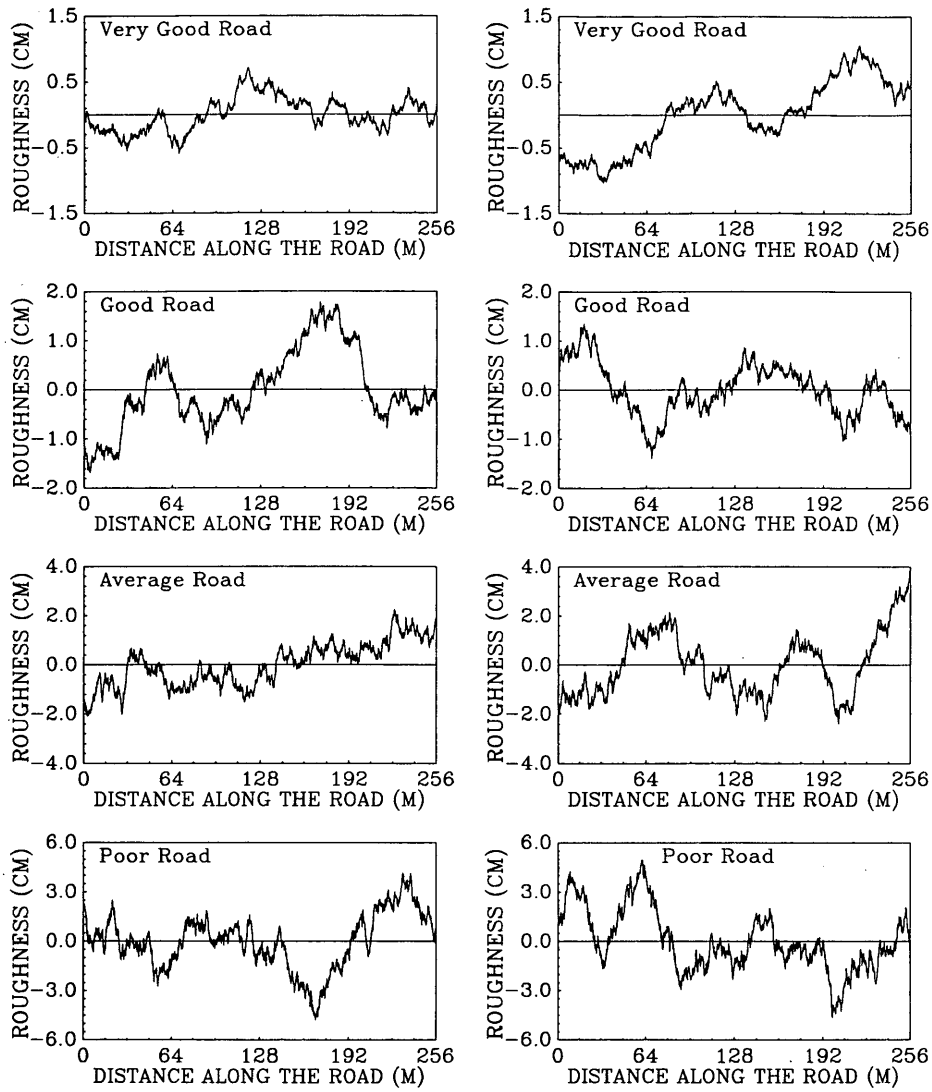

FIGURE 2 Vertical highway surface profiles: *left*, right line; *right*, left line.

VIBRATION AND IMPACT CHARACTERISTICS

It is assumed that the bridges have damping characteristics that can be modeled as viscous. One percent of critical damping is adopted for the first and second modes according to the experiment results. The mode-damping coefficients were determined by using an approach described by Clough and Penzien (*18*). To obtain the initial displacements and velocities of vehicle degrees of freedom when the vehicle entered the bridge, the vehicle was started in motion at a distance of 140 ft (42.67 m, i.e., a five-car length) away from the left end of the bridge and continued moving until the entire vehicle cleared the right end of the bridge. The same class of road surface was assumed for both the approach roadways and bridge decks.

Table 2 presents the first six frequencies of each bridge. From the table, it is apparent that the first two frequencies of each bridge—corresponding with bending and torsion modes, respectively—are nearly the same.

To learn the space impact characteristics of multigirder bridges, two loading cases, symmetric and asymmetric loadings of a single truck [Figure 6 (*top*) Loading 1 and Loading 2], are considered. Under the conditions of vehicle speed of 45 mph (72.41 km/hr) and good road surface, the lateral wheel-load distribution factors and impact factors of three bridges with span lengths of 35, 55, and 100 ft (10.67, 16.75, and 30.48 m), respectively, are computed and shown in Figure 7. The wheel-load distribution factor acquired for the study is defined as

$$\eta = F_{MQi}/F_{MQt} \tag{6}$$

where

$F_{MQt} = F_{MQ}/n$

F_{MQ} = sum of bending moment or shear of all girders at one section,

n = number of wheel-loads in transverse direction, and

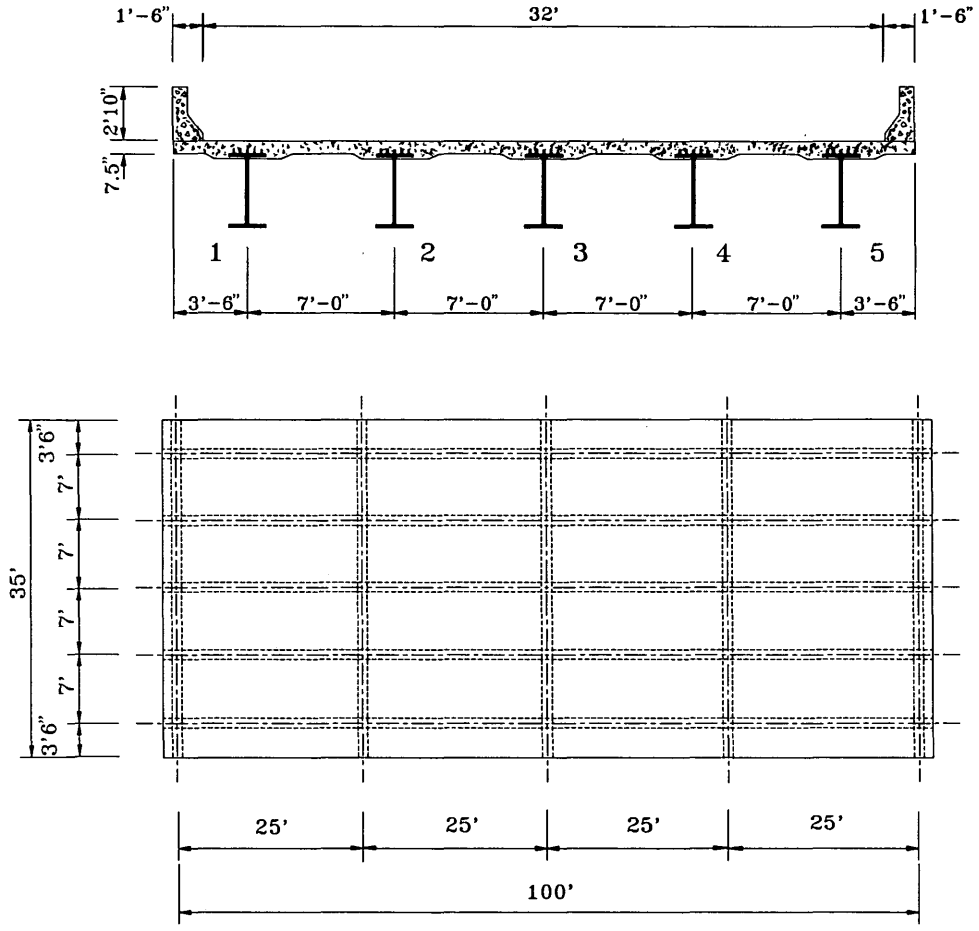

FIGURE 3 Typical analytical bridge: *top*, typical cross section; *bottom*, typical plan.

TABLE 1 Properties and Masses of Bridges

Span length ft	Girder				Intermediate diaphragm			Diaphragm at ends		
	I^{*} x 10^4 (in^4)	J_d^{**} x 10^3 (in^4)	Mass (kips/in)		I^{*} x 10^4 (in^4)	J_d^{**} x 10^3 (in^4)	Mass (kips/in)	I^{*} x 10^4 (in^4)	J_d^{**} x 10^3 (in^4)	Mass (kips/in)
			Exterior girder	Interior girder						
35	1.209	1.792	0.0927	0.0661	0.211	0.498	0.0027	0.211	0.498	0.0027
45	1.659	1.792	0.0941	0.0676	0.225	0.640	0.0027	0.225	0.640	0.0027
55	2.352	1.799	0.0967	0.0701	0.355	0.783	0.0027	0.228	0.782	0.0035
75	3.734	1.830	0.1052	0.0787	0.367	1.066	0.0027	0.256	1.065	0.0035
100	8.002	1.797	0.0991	0.0725	0.981	1.420	0.0057	1.852	1.420	0.0031
120	10.688	1.801	0.1037	0.0776	1.222	1.705	0.0064	2.802	1.704	0.0038
140	15.475	1.805	0.1078	0.0812	1.765	1.989	0.0064	3.965	1.988	0.0038

* Inertia moment.

** Torsional inertia moment.

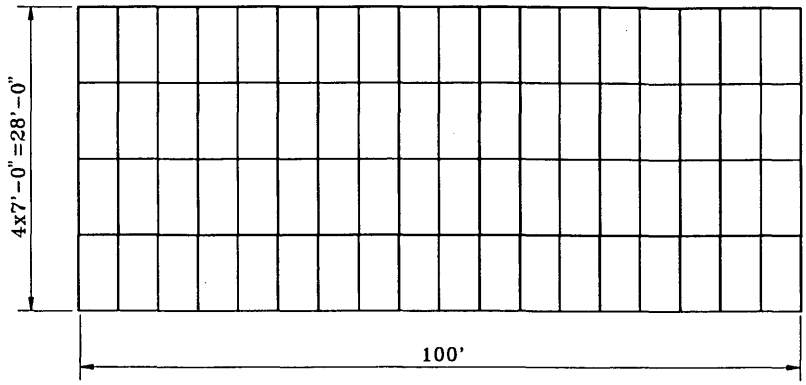

FIGURE 4 Idealization of multigirder bridges.

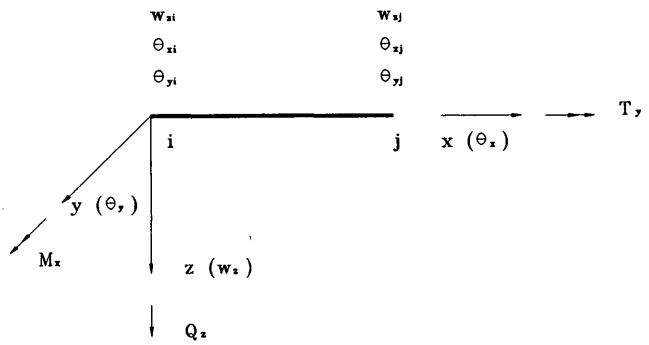

FIGURE 5 Grillage elements.

F_{MQi} = maximum bending moment or shear of one girder at the section.

The impact factor is defined as

$$I_{mp}(\%) = [R_d/R_s - 1] \times 100\% \quad (7)$$

in which R_d and R_s are the absolute maximum response for dynamic and static studies, respectively.

Figure 7 (*left*) presents the static load distribution factors and impact factors of each girder for the three bridges subjected to lateral symmetrical loading of a single truck. It is interesting to observe from Figure 7 (*left*) that lateral static and dynamic load distributions are quite different, especially for short-span bridges. The larger the static lateral load distribution factor is, the smaller the impact factor will be. The impact factors of exterior girders are much larger than those of interior girders. Therefore, taking an average impact factor of all girders as that of each girder in the theoretical and field study is not reasonable. However, the difference of impact factors between exterior and interior girders will decrease with the increase of span length.

Figure 7 (*right*) shows the results for the case of asymmetrical loading of a single truck. The same relation between static wheel-load distribution factor and impact factor will be observed from Figure 7 (*right*). However, because of the effect of torsion, the impact factors of Girders 1 to 3 have nearly the same value.

Figure 8 gives the variation of the impact factors of moment at midspan for exterior and center girders of three bridges with varying vehicle weight. The results in Figure 8 were based on the conditions of a single truck loading symmetrically [Figure 6 (*top*), Loading 1], 45-mph (72.41-km/hr) vehicle speed, and good road surface. Figure 8 shows the impact factor increases as the weight decreases. However, the relation between impact and vehicle weight is related to different span lengths, girders, and cross sections. The shorter the span length is, the more rapidly the impact factor will increase with less-

TABLE 2 Frequencies of Seven Bridges

No. of frequency	Span length (ft)						
	35	45	55	75	100	120	140
1	11.657	8.231	6.467	4.185	3.502	2.791	2.410
2	11.754	8.368	6.588	4.327	3.526	2.814	2.411
3	16.882	13.247	12.967	10.131	13.368	10.647	9.152
4	31.096	26.877	24.970	16.256	13.617	11.186	9.694
5	44.844	31.713	25.282	16.533	13.961	13.956	15.488
6	44.854	31.729	29.996	20.054	18.767	17.796	17.654

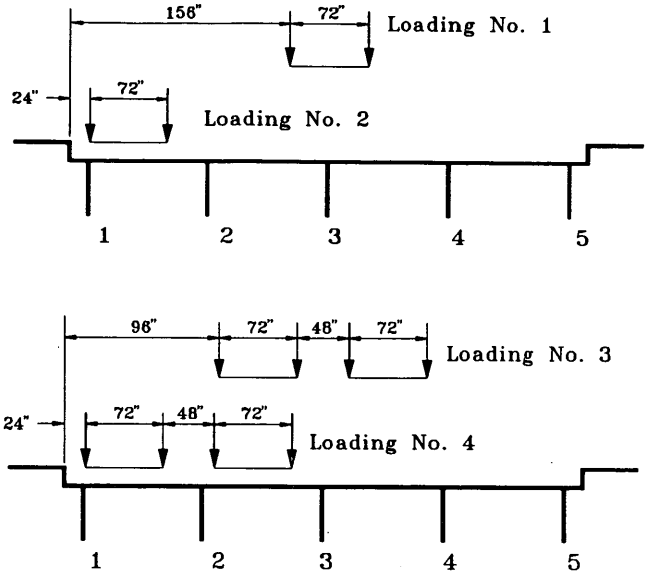

FIGURE 6 Truck-loading model: *top*, one-truck loading; *bottom*, two-truck loading.

ening vehicle weight; the impact factors of exterior girders increase much faster than those of center girders.

Figure 9 illustrates the variation of the maximum impact factor with varying span length for two typical sections of midspan and span fourth point. Figure 9 (*left*) represents the response of exterior girders, while that of center girders is given in Figure 9 (*right*). The maximum impact factors were obtained on the basis of the transverse position that can produce the maximum static response in the girders concerned (see Figure 6) and vehicle speeds ranging from 15 to 75 mph (24.14 to 120.68 km/hr).

Figure 9 provides important information concerning the relationship among maximum impact factor, span length, and others. For all seven bridges, the maximum impact factors of exterior girders are apparently larger than those of center girders. Generally, the impact factors of moment of exterior girders for bridges with span length in excess of 60 ft (18.29 m) are distinctly smaller than those evaluated according to Equation 1, provided that bridges have a deck of good road surface roughness. Higher impact factors will occur in the bridges with short spans, for which the AASHTO specifications may underestimate the impact of exterior girders. Nevertheless, the impact factors of center girders of the seven bridges with good road surface are all smaller than those predicted by Equation 1. It seems that Equation 1 will overestimate the impact of center girders for the bridges whose span lengths are in excess of 55 ft (16.76 m). The variation of the impact factors of moment at span fourth point with span lengths is different from that at midspan. For the bridges with short span lengths and very good roughness, the impact factors at span fourth point are generally less than those at midspan. For the opposite situation, most impact factors at span fourth point are greater than those at midspan. Figure 9 also shows that the impact of bridges increases considerably with increasing road roughness.

CONCLUSIONS

1. The impact of each girder of steel multigirder bridges is closely related to the lateral loading position of vehicles. Lateral static and dynamic distributions of the bridges are quite different, especially for short-span bridges. The larger the static lateral distribution factor is, the smaller the impact factor will be. It appears more reasonable to study the maximum

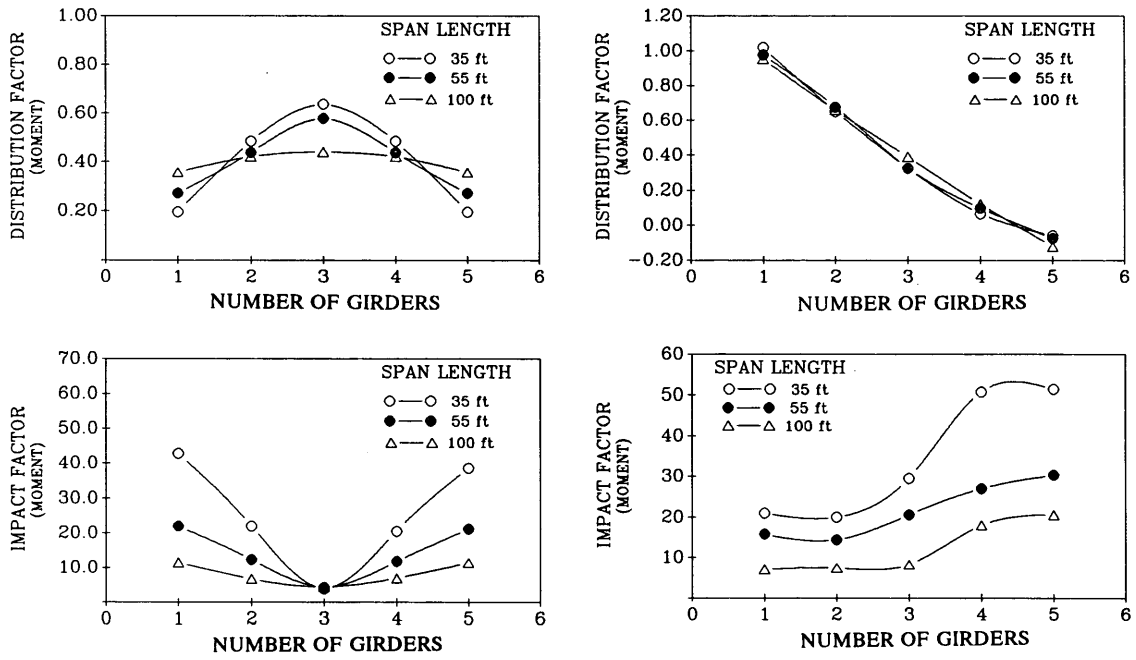

FIGURE 7 Static and dynamic distribution: *left*, symmetric loading; *right*, asymmetric loading.

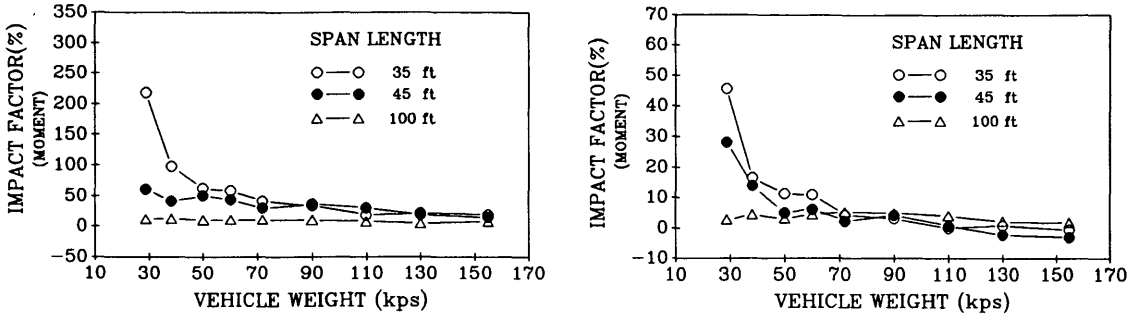

FIGURE 8 Effect of vehicle weight: *left*, exterior girders; *right*, center girders.

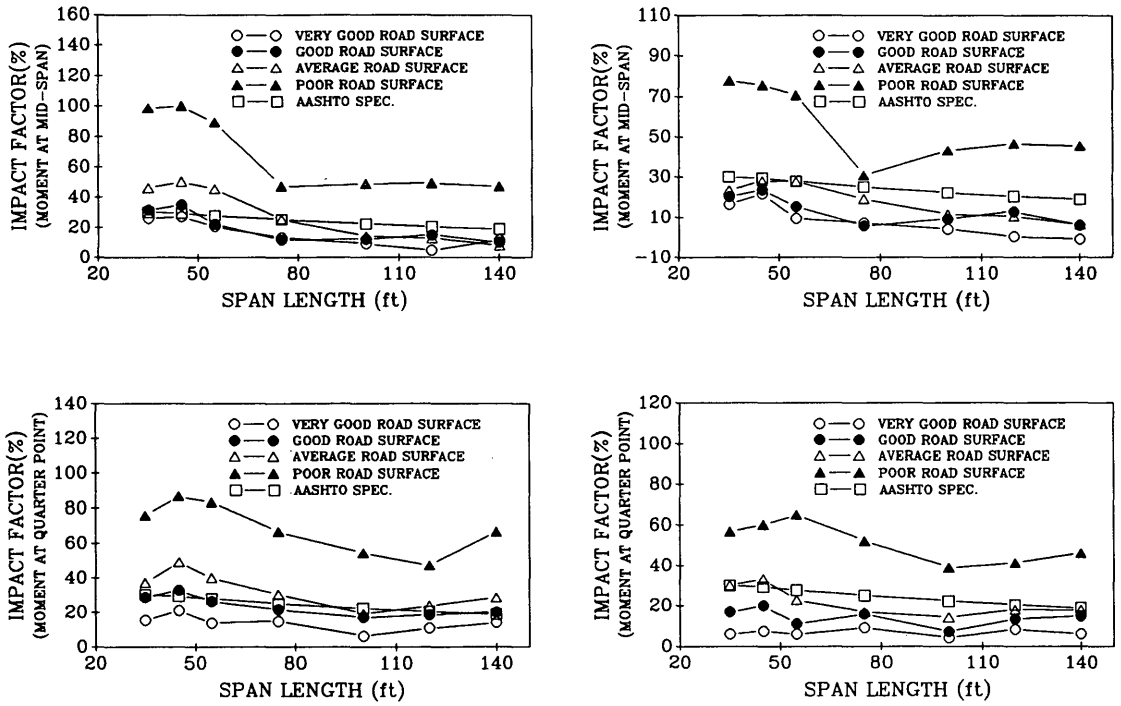

FIGURE 9 Variation of maximum-impact factors with span lengths: *left*, exterior girders; *right*, center girders.

impact of each girder than to adopt the average value of all girders in field investigations, particularly for short-span bridges.

2. Impact factors of bridges decrease with increasing vehicle weight. However, the relation between the impact and the weight of vehicle is correlated with different span lengths, girders, and sections. The shorter the span length is, the more rapidly the impact factor will increase with lessening vehicle weight. The impact factors of exterior girders increase faster than those of interior girders.

3. The maximum impact factors of interior girders for all seven bridges are significantly smaller than those of exterior girders and less than the results calculated by AASHTO specifications, provided that the bridges have good road surface. It appears that Equation 1 will overestimate the maximum factors of moment for bridges with span lengths longer than 55 ft (16.76 m), especially for midspan.

4. Generally, the maximum impact factors of moment of exterior girders with span lengths longer than 75 ft (22.86 m) are distinctly lower than those predicted by AASHTO specifications, provided that bridges have good road surface. For bridges with short spans, it appears that Equation 1 may underestimate impact value. This situation should be noted in practice.

REFERENCES

1. *Standard Specifications for Highway Bridges*, 14th ed. AASHTO, Washington, D.C., 1989.
2. *Ontario Highway Bridge Design Code*. Ministry of Transportation and Communications, Ontario, Canada, (1983).
3. D. R. Leonard, J. W. Grainger, and R. Eyre. *Loads and Vibrations Caused by Eight Commercial Vehicles with Gross Weights Exceeding 32 Tons*. Laboratory Report LR52. Transport and Road Research Laboratory, Crowthorne, England, 1974.
4. J. Page. *Dynamic Wheel Load Measurements on Motorway Bridges*. Laboratory Report LR 722. Transport and Road Research Laboratory, Crowthorne, England, 1976.

5. R. Shepard and R. J. Aves. Impact Factors of Simple Concrete Bridges. *Proc., Institution of Civil Engineering*, Part 2, Vol. 55, 1973, pp. 191–210.
6. R. Green. *Dynamic Response of Bridge Superstructures—Ontario Observations*. Supplementary Report 275. Transport and Road Research Laboratory, Crowthorne, England, 1977, pp. 40–48.
7. C. O'Connor and R. W. Pritchard. Impact Studies on Small Composite Girder Bridge. *Journal of Structural Engineering*, ASCE, Vol. 116, No. 7, 1985.
8. T. Huang. *Dynamic Response of Three-Span Continuous Highway Bridges*. Ph.D. dissertation. University of Illinois, Urbana, 1960.
9. R. K. Gupta and R. W. Trail-Nash. Vehicle Braking on Highway Bridges. *Journal of the Engineering Mechanics Division*, ASCE, Vol. 106, No. EM4, 1980, 641–658.
10. C. Oran. *Analysis of the Static and Dynamic Response of Single-Span Multigirder Highway Bridges*. Ph.D. dissertation. University of Illinois, Urbana, 1961.
11. E. S. Hwang and A. S. Nowak. Simulation of Dynamic Load for Bridges. *Journal of Structural Engineering*, ASCE, Vol. 117, No. 5, pp. 1413–1434.
12. T. L. Wang and D. Z. Huang. Cable-Stayed Bridge Vibration Due to Road Surface Roughness. *Journal of Structural Engineering*, ASCE, Vol. 118, No. 5, 1992, pp. 1354–1374.
13. T. L. Wang and D. Z. Huang. *Computer Modeling Analysis in Bridge Evaluation*. Interim Research Report FL/DOT/RMC/0542-3394. Florida Department of Transportation, Tallahassee, 1992.
14. C. J. Dodds. and J. D. Robson. The Description of Road Surface Roughness. *Journal of Sound and Vibration*, Vol. 31, No. 2, 1973, pp. 175–183.
15. C. J. Dodds. *BSI Proposals for Generalized Terrain Dynamic Inputs to Vehicles*. ISO/TC/108/WG9, Document 5. International Organization for Standardization, 1972.
16. *Standard Plans for Highway Bridge Superstructures*. FHWA, U.S. Department of Transportation, 1982.
17. T. L. Wang. Ramp/Bridge Interface in Railway Prestressed Concrete Bridges. *Journal of Structural Engineering*, ASCE, Vol. 116, No. 6, 1990, pp. 1648–1659.
18. R. W. Clough and J. Penzien. *Dynamics of Structures*. McGraw-Hill Book Co., New York, N.Y., 1975.

Publication of this paper sponsored by Committee on Steel Bridges.